Quantum Dots

DOI: 10.1002/anie.200503152

Enhanced Collective Electron Transport by CdSe Quantum Dots Confined in the Poly(4-vinylpyridine) Nanodomains of a Poly(styrene-*b*-4-vinylpyridine) Diblock Copolymer Thin Film**

Chung-Ping Li, Kung-Hwa Wei, and Jung Y. Huang*

Semiconductor nanoparticle (NP) quantum dots (QDs) that have sizes close to their Bohr exciton radius (typically between 1 and 10 nm) display size-dependent band gaps and hence tunable optical properties.[1] As a result, they exhibit a wide range of electrical and optical properties and can be used for various applications, such as light-emitting diodes, solar cells, lasers, and transistors. In these applications, composite materials consisting of nanoparticles and organic materials are often adopted. Thus, an understanding of the collective

[*] C.-P. Li, Prof. K.-H. Wei
Department of Materials Science and Engineering
National Chiao Tung University
1001 Ta Hsueh Road, Hsinch 30050 (Taiwan ROC)
Fax: (+886) 35-724-727
E-mail: khwei@cc.nctu.edu.tw
Prof. J. Y. Huang
Department of Electro-Optical Engineering
National Chiao Tung University
1001 Ta Hsueh Road, Hsinch 30050 (Taiwan ROC)

[**] The authors acknowledge the National Science Council in Taiwan for funding (NSC 94-2120M-009-001).

Supporting information for this article is available on the WWW under http://www.angewandte.org or from the author.

electron transport of QDs dispersed in organic materials is of both scientific and technological importance. A number of reports have described three- and two-dimensional electron transport in ordered arrays of Au NPs in SiO_2 superlattices,[2] ZnO QD assemblies,[3] and organically capped CdSe QDs.[4] Electron transport also has been examined in granular films of Au NPs linked by alkanethiol molecules[5] or poly(4-vinylpyridine)[6] and Au/spacer/CdSe QD[7] assemblies. Orbital-selective electron transport through a single CdSe QD has been measured by scanning tunneling microscopy.[8]

Thin films of diblock copolymers are versatile templates for the preparation of long-range-ordered arrays of nanostructures, because their periodic thickness can be tuned between 10 and 100 nm.[9] For example, the selective sequestration of presynthesized CdS,[10a] CdSe,[11] and TiO_2[10b] nanoparticles into one block of a diblock copolymer is performed through strong interactions between one block of the copolymer and the surface ligands of the nanoparticles. Encapsulation of Au nanoparticles in a block copolymer has also been reported.[12] In the present study, we prepared self-assembled thin films that consisted of CdSe QDs sequestered in the poly(4-vinylpyridine) nanodomains of poly(styrene-*b*-4-vinylpyridine) (S4VP) diblock copolymer, following a previously reported approach.[10] By conductive atomic force microscopy (C-AFM) and measurements on devices, we found that the electron-tunneling rate constant of CdSe QDs confined in poly(4-vinylpyridine) nanodomains is much larger than that in a random distribution. To our knowledge, this is the first report on the nanodomain-confinement effect on the collective electron-transport behavior of quantum dots. This has large implications for application in hybrid photovoltaic cells and light-emitting diodes, because collective electron transport by CdSe QDs and hole transport by organic materials, respectively, are critical for producing highly efficient hybrid photovoltaic cells[1] and light-emitting diodes.[13]

Figure 1 shows the process for preparing a monolayered (CdSe/P4VP)-*b*-PS thin film. First, the trioctylphosphine oxide (TOPO) ligands on the CdSe QDs were exchanged by hydrophilic pyridine ligands. Then, pyridine-modified CdSe QDs and PS-*b*-P4VP block copolymer were dissolved and mixed in pyridine, whereby the CdSe QDs are distributed selectively in the P4VP phase due to dipole–dipole interactions. After drying, (CdSe/P4VP)-*b*-PS in bulk form was obtained. Subsequently, toluene, which is a good solvent for PS but a poor one for P4VP, was used to form a solution containing micelles with CdSe/P4VP cores and PS shells. The micellar solutions were then spin-coated at 5000 rpm for 60 s on carbon-coated silicon wafers to form thin films for transmission electron microscopy study and device measurements, respectively. Figure 2a shows a transmission electron microscopy (TEM) image of a thin film of 48% (CdSe/P4VP)-*b*-PS recorded without staining. The dark regions

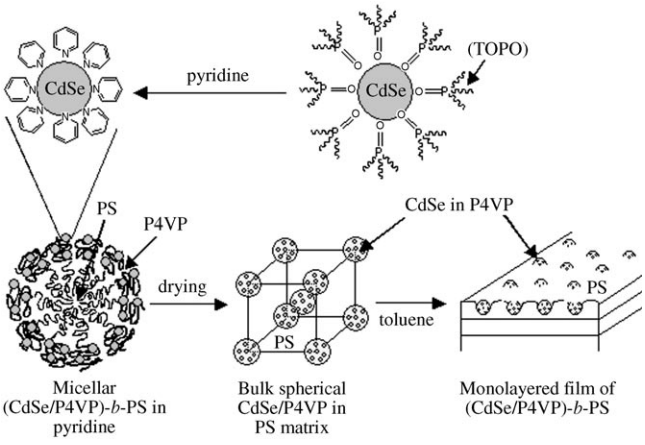

Figure 1. Preparation of a monolayered (CdSe/P4VP)-*b*-PS thin film by incorporation of selectively dispersed pre-synthesized CdSe QDs in P4VP domains.

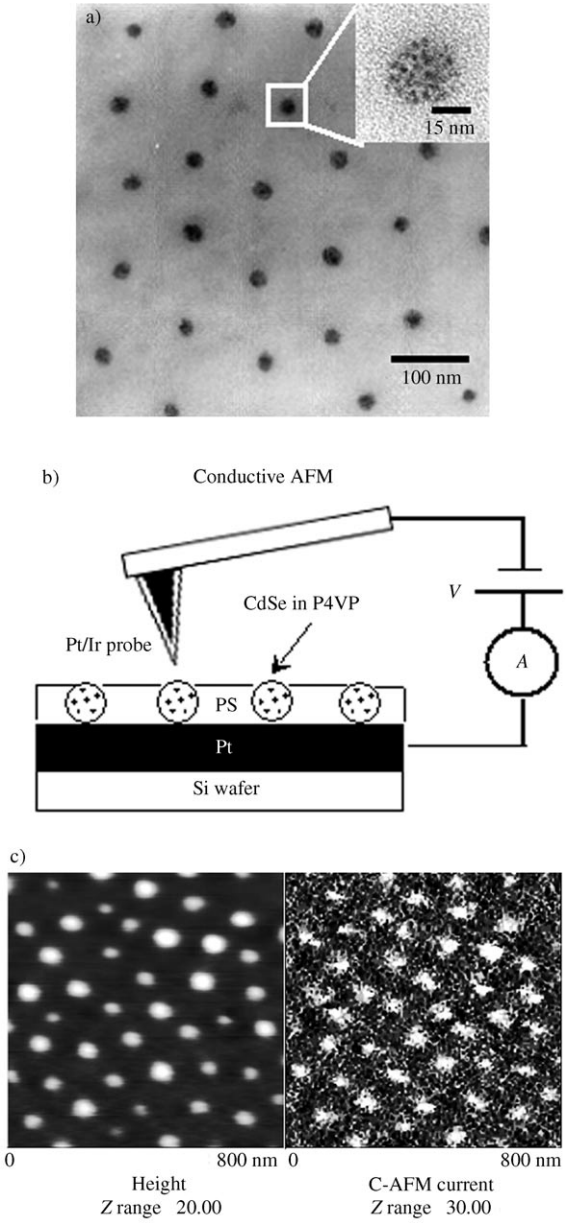

Figure 2. a) TEM image of a thin film of 48% (CdSe/P4VP)-*b*-PS obtained without staining. b) Schematic representation of the C-AFM imaging mode. c) C-AFM topographic (left) and current (right) images of a thin film of 48% (CdSe/P4VP)-*b*-PS.

show the CdSe/P4VP composite phase representing the higher electron density of cadmium. The PS-*b*-P4VP nanospheres are thus revealed clearly. The diameter of the CdSe/P4VP spheres is about 35 nm, and the interdomain distance about 100 nm. The inset of Figure 2a reveals that CdSe QDs are dispersed homogeneously in a P4VP nanodomain. Figure 2b shows a schematic representation of the C-AFM method we used to analyze the CdSe/P4VP spheres embedded in polystyrene. The current image was measured at a sample bias of $V_B = 8$ V. Figure 2c shows the topographic and current images of a section of the thin film of 48% (CdSe/P4VP)-*b*-PS. In the height image, the light regions with a size of about 35 nm represent the CdSe/P4VP domains, and the dark area the polystyrene matrix. Because the thickness of the film is smaller than the size of the CdSe/P4VP domains (23 vs 30 nm), this image indicates that microphase-separated (CdSe/P4VP)-*b*-PS exists as a monolayered thin film. In the current image, the currents of the P4VP/CdSe phases (light regions) were about 30–40 pA, whereas that of the PS phase (dark regions) was at the level of the noise (ca. 0.5 pA).

Figure 3a displays the current–voltage (*I*–*V*) curves of a single CdSe/P4VP nanodomain, as measured by C-AFM. The turn-on voltage of the CdSe/P4VP nanodomains decreases with increasing number of incorporated CdSe QDs. This phenomenon occurs because the electron mobility from the probe to the nanodomains increases with increasing density of CdSe QDs. The linear regions of the *I*–*V* curves represent Ohmic behavior[17] and indicate constant conductivities σ that can be calculated from the slope of the curves.[14] The nonlinear regions are due to electron tunneling from the probe tip to the conduction band of CdSe QDs, which must overcome the barrier height ϕ_e of the P4VP between the tip and CdSe (inset of Figure 3a).[14,19] A tunneling process in which electron injection occurs under a forward bias can be properly modeled by using the Fowler–Nordheim (FN) equation to determine the electron barrier height ϕ_e.[14] The ϕ_e values for the 10, 15, 26, 33, and 48% CdSe QDs in the P4VP block were 2.4, 2.2, 2.0, 1.8, and 1.5 eV, respectively.[14] The ϕ_e value decreases monotonically with increasing amount of CdSe QDs in the P4VP block because the distance between the tip and CdSe QDs decreases at higher densities of CdSe QDs. Figure 3b shows the conductivity of a single CdSe/P4VP nanodomain as a function of the volume fraction of incorporated CdSe in P4VP. The conductivity of the CdSe/P4VP nanodomain displays only a slight change at low CdSe loadings, exhibits a sharp increase at a critical loading, and becomes saturated at high loading. Hence, the conductivity of polymers incorporating CdSe QDs is best described by a percolation theory (the solid curve in Figure 3b represents the best fit to the experimental data).[14] The conductivity σ of a single CdSe/P4VP nanodomain is on the order of 10^{-5} to $10^{-7}\ \Omega^{-1}\,cm^{-1}$ (Table 1). The conductivity increases with increasing amount of CdSe because the distance between CdSe QDs decreases at higher densities of CdSe QDs. We also obtained the averaged current–voltage (I_{av}–*V*) curve of a single CdSe/P4VP nanodomain in PS matrix in a sandwich device.[14] The conductivity of the device also increases with increasing amount of CdSe and is on the same order of magnitude (10^{-7} to $10^{-5}\ \Omega^{-1}\,cm^{-1}$) as that measured by C-AFM (Table 1).

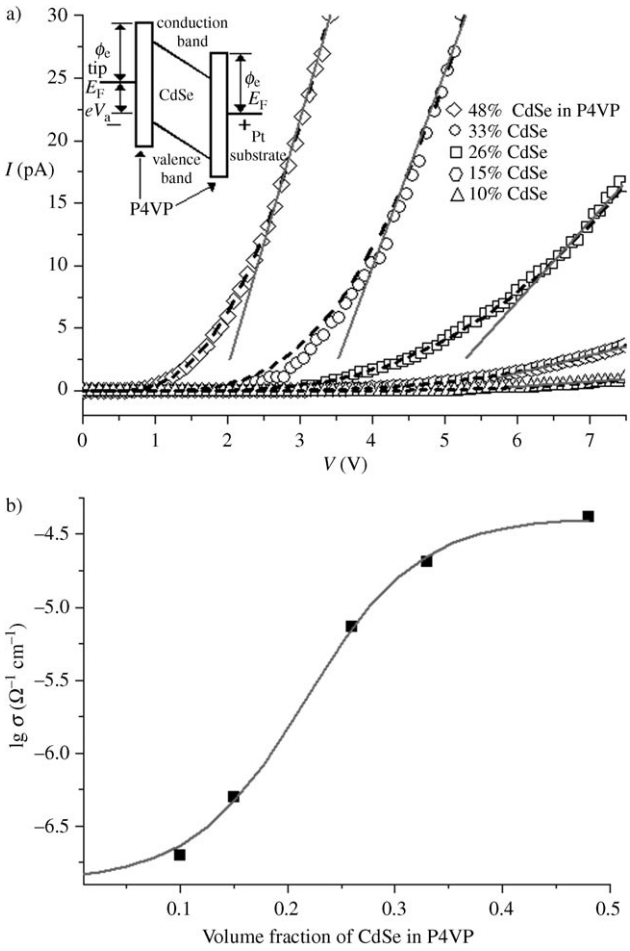

Figure 3. a) *I*–*V* curves of a single CdSe/P4VP nanodomain in (CdSe/P4VP)-*b*-PS thin films, as measured by C-AFM. The dotted lines are best fits of the FN equation. Inset: The energy bands of the C-AFM tip, CdSe/P4VP monolayer, and substrate. E_F is the electron Fermi energy inside Pt, and ϕ_e is the barrier height between Pt and CdSe/P4VP. eV_a is the applied potential energy difference between the tip and the substrate. b) Plot of conductivity versus amount of CdSe in P4VP.

Table 1: Conductivity σ and electron-tunneling rate constant k_{ET} for nanodomain-confined and randomly distributed CdSe in P4VP, as measured by C-AFM and in a device.

CdSe in P4VP [vol%]	$10^6\sigma$ [$\Omega^{-1}\,cm^{-1}$]				$10^{-3}\,k_{ET}$ [s^{-1}]			
	(CdSe/P4VP)-*b*-PS (nanodomain-confined)		CdSe/P4VP (randomly distributed)		(CdSe/P4VP)-*b*-PS (nanodomain-confined)		CdSe/P4VP (randomly distributed)	
	C-AFM	device	C-AFM	device	C-AFM	device	C-AFM	device
10	0.2	0.13	0.03	0.01	1.4	0.9	0.2	0.09
15	0.6	0.46	0.08	0.05	4.2	3.2	0.5	0.4
26	7.4	5.2	0.82	0.6	39	27	4.3	3.1
33	20	14	2.2	1.6	87	60	9.6	6.9
48	41	28	4.8	2.9	179	127	21.3	13.2

Figure 4a shows a plot of $-\ln\sigma$ versus the edge-to-edge interparticle distance δ_e, as measured by C-AFM and in a device. The conductivity in terms of δ_e and temperature T is described[5,15] by Equation (1) where σ is the conductivity of

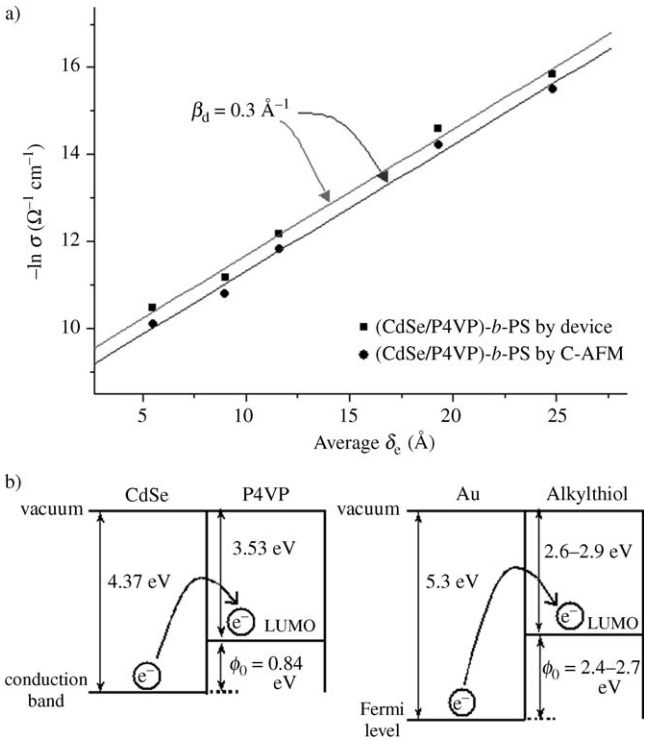

Figure 4. a) Plot of $-\ln\sigma_{(CdSe/P4VP)\text{-}b\text{-}PS}$ versus δ_e, as measured by C-AFM and in a device. b) Schematic diagram of the barrier height for electron tunneling from the conduction band of CdSe to the LUMO of P4VP[18] and from the Fermi level of Au to the LUMO of an alkanethiol.[15,16]

the resulting composite, β_d the electron-tunneling coefficient, δ_e the edge-to-edge interparticle distance,[14] E_A the activation barrier energy, R the gas constant, and T the temperature.

$$\sigma(\delta_e,T) = \sigma_0 \exp[-\beta_d \delta_e]\exp\left[\frac{-E_A}{RT}\right] \quad (1)$$

The linear slope of the plot of $-\ln\sigma$ versus δ_e indicates an electron-hopping mechanism, and the value of the slope (i.e., β_d) is 0.3 Å^{-1}. In our system, the value of β_d differs from that found in other cases. For instance, the value of β_d is 0.2–0.6 Å^{-1} for electron tunneling through π-bonded molecules, and about 0.6–1.0 Å^{-1} for saturated molecules.[16] The electron-tunneling coefficient β_d can be described[16] by Equation (2) where m^* is the electron effective mass, ϕ_0 the electron-tunneling barrier height between the dots, and $\hbar$ the reduced Planck constant.

$$\beta_d = 2\sqrt{\frac{2m^*\phi_0}{\hbar^2}} \quad (2)$$

Electron tunneling from one dot to the next must overcome the tunneling barrier height ϕ_0 of the spacer between the two dots. We found that the value of β_d in the CdSe–P4VP–CdSe system (0.3 Å^{-1}) is small when compared to that in the Au–alkanethiol–Au system (0.8–1.2 Å^{-1}), because the tunneling barrier height between the conduction band of CdSe and the LUMO of P4VP is smaller than that between the Fermi level of Au and the LUMO of an alkanethiol (Figure 4b).[5,6] The smaller β_d value for (CdSe/P4VP)-*b*-PS than for Au–alkanethiol indicates that the edge-to-edge interparticle distance has less effect on the conductivity for (CdSe/P4VP)-*b*-PS than for the Au–alkanethiol–Au system. The effective electron mass $m^* = 0.14m$ was calculated by Equation (2), where m is the free electron mass.

To compare the effect that nanodomain confinement has on the CdSe QDs with respect to their randomly distributed state, we prepared four samples that had the same density of P4VP: the first two contained 48 vol% CdSe with respect to the P4VP blocks in a PS-*b*-P4VP diblock copolymer, and the second two contained 48 vol% CdSe in a P4VP homopolymer. The electron-tunneling rate constant k_{ET} can be estimated from the conductivity by assuming a cubic-lattice model described by an equation.[5,14] Table 1 indicates that both k_{ET} and σ for the nanodomain-confined case are about seven times larger than those for the randomly distributed case. This can be explained by the fact that the collective electron transport of CdSe QDs in the nanodomain-confined case is restricted by the P4VP sphere, while the collective electron transport for the randomly distributed CdSe QDs follows a free-pathway behavior. The k_{ET} value increases with increasing amount of CdSe.

In conclusion, we have demonstrated that the electron-tunneling rate constant of CdSe QDs confined in a poly(4-vinylpyridine) nanodomain is much larger than that in a random distribution, and it increases with increasing amount of CdSe. The electron-tunneling coefficient of the CdSe–P4VP–CdSe system is 0.3 A^{-1}. The electron barrier height from the tip of the probe to the nanodomain decreases monotonically and the conductivity of the CdSe/P4VP nanodomain increases in accordance with a percolation model with increasing amount of CdSe.

Received: September 6, 2005
Revised: November 24, 2005
Published online: January 30, 2006

Keywords: block copolymers · electron transport · monolayers · quantum dots · semiconductors

[1] W. Huynh, J. J. Dittmer, A. P. Alivisatos, *Science* **2002**, *295*, 2425–2427.
[2] H. Fan, K. Yang, D. M. Boye, T. Sigmon, K. J. Malloy, H. Xu, G. P. Lopez, C. J. Brinker, *Science* **2004**, *304*, 567–571.
[3] a) A. L. Roest, J. J. Kelly, D. Vanmaekelbergh, *Phys. Rev. Lett.* **2002**, *89*, 036801; b) A. L. Roest, J. J. Kelly, D. Vanmaekelbergh, *Appl. Phys. Lett.* **2003**, *83*, 5530–5532.
[4] D. Yu, C. Wang, P. Guyot-Sionnest, *Science* **2003**, *300*, 1277–1280.
[5] W. P. Wuelfing, S. J. Green, J. J. Pietron, D. E. Cliffel, R. W. Murry, *J. Am. Chem. Soc.* **2000**, *122*, 11465–11472.
[6] R. J. Forster, L. Keane, *J. Electroanal. Chem.* **2003**, *554–555*, 345–354.

[7] E. P. A. M. Bakkers, A. W. Marsman, L. W. Jenneskens, D. Vanmaekelbergh, *Angew. Chem.* **2000**, *112*, 2385 – 2388; *Angew. Chem. Int. Ed.* **2000**, *39*, 2297 – 2299.
[8] E. P. A. M. Bakkers, Z. Hens, A. Zunger, A. Franceschetti, L. P. Kouwenhoven, L. Gurevich, D. Vanmaekelbergh, *Nano Lett.* **2001**, *1*, 551 – 556.
[9] J. P. Spatz, S. Mossmer, C. Hartmann, M. Möller, T. Herzog, M. Krieger, H. G. Boyen, P. Ziemann, B. Kabius, *Langmuir* **2000**, *16*, 407 – 415.
[10] a) S. W. Yeh, K. H. Wei, Y. S. Sun, U. S. Jeng, K. S. Liang, *Macromolecules* **2003**, *36*, 7903 – 7907; b) C. C. Weng, K. H. Wei, *Chem. Mater.* **2003**, *15*, 2936 – 2941; c) S. W. Yeh, T. L. Wu, K. H. Wei, *Nanotechnology* **2005**, *16*, 683 – 687; d) C. C. Weng, C. P. Chen, C. H. Ting, K. H. Wei, *Chem. Mater.* **2005**, *17*, 3328 – 3330.
[11] Y. Lin, A. Böker, J. He, K. Sill, H. Xiang, C. Abetz, X. Li, J. Wang, T. Emrick, S. Long, Q. Wang, A. Balazs, T. P. Russell, *Nature* **2005**, *434*, 55 – 59.
[12] Y. Kang, T. A. Taton, *Angew. Chem.* **2005**, *117*, 413 – 416; *Angew. Chem. Int. Ed.* **2005**, *44*, 409 – 412.
[13] N. Tesster, V. Medvedev, M. Kazes, S. Kan, U. Banin, *Science* **2002**, *295*, 1506.
[14] See the Supporting Information.
[15] F. P. Zamborini, L. E. Smart, M. C. Leopold, R. W. Murry, *Anal. Chim. Acta* **2003**, *496*, 3 – 16.
[16] a) A. Salomon, D. Cahen, S. Lindsay, J. Tomfohr, V. B. Engelkes, C. D. Frisbie, *Adv. Mater.* **2003**, *15*, 1881 – 1890; b) X. D. Cui, X. Zarate, J. Tomfohr, O. F. Sankey, A. Primak, A. L. Moore, T. A. Moore, D. Gust, G. Harris, S. M. Lindsay, *Nanotechnology* **2002**, *13*, 5 – 14.
[17] N. Boden, R. J. Bushby, J. Clements, B. Movaghar, *J. Appl. Phys.* **1998**, *83*, 3207 – 3216.
[18] We measured the HOMO and LUMO levels of P4VP by cyclic voltammetry (CV).
[19] D. Xu, G. D. Watt, J. N. Harb, R. C. Davis, *Nano Lett.* **2005**, *5*, 571 – 577.

